High-resolution study of conductivity and cell potential versus doping concentration in potassium-doped polyacetylene: Correlation with structural transitions

N. Coustel and P. Bernier
Groupe de Dynamique des Phases Condensees, Université des Sciences et Techniques du Languedoc, Place Eugène Bataillon, 34095 Montpellier CEDEX 5, France

J. E. Fischer
Materials Science and Engineering Department and Laboratory for Research on the Structure of Matter, University of Pennsylvania, Philadelphia, Pennsylvania 19104-6272

(Received 27 July 1990)

A high-resolution quasiequilibrium *in situ* study of parallel conductivity $\sigma_{\parallel}$ and open-circuit voltage V_{OC} during potassium doping and dedoping of an oriented $(CH)_x$ electrode is presented. Features in dV_{OC}/dy and $d\sigma_{\parallel}/dy$ (y=K mole fraction) found previously at $y=0.06$, 0.12, and 0.15 are confirmed and correlated with recent x-ray and ESR results and with a model of staging via intercalation channels. We also find new features during dedoping at $y=0.03$ and 0.08 in $d\sigma_{\parallel}/dy$ but not in dV_{OC}/dy, the former coinciding with a similar ESR feature. We propose that these are signatures of subtle structural effects that do not involve major changes in lattice constants or unit-cell symmetries. We tentatively assign the $y=0.03$ feature to a metastable "dilute stage-2" phase, by analogy to graphite intercalates. Similarly, three phases with the same stage-1 channel structure are inferred from the observation of three plateaus in $V_{OC}(y)$ in the range $0.10<y<0.17$ upon dedoping. A maximum $\sigma_{\parallel}=17\,500$ S/cm is found near $y=0.12$ during the first doping cycle. With successive cycles $\sigma_{\parallel}$(max) decreases, the maximum attainable y also decreases, and $V_{OC}(y)$ approaches the ideal behavior of an intercalation electrode exhibiting first-order phase transitions.

INTRODUCTION

Polycetylene $(CH)_x$ exhibits spectacular and reversible changes in electronic properties (conductivity, ESR, susceptibility) during doping and dedoping with electron donors or acceptors. The overall conductivity variation is usually discussed in terms of several distinct phenomena: soliton doping of the insulating host material up to 6 at. %, followed by a metallic regime in which the conductivity versus dopant mole fraction y reflects the competition between increasing free-electron concentration and enhanced electron-phonon scattering as the Fermi surface grows.[1] It is also believed that interchain coupling is crucial for the intrachain electron transport; since the chains contain defects and are of finite length, a carrier must be able to hop from chain to chain in order to contribute to the macroscopic current. Recent x-ray results on $[(CH)K_y]_x$ show that, to these, the possible influence of structural transitions versus y must be added,[2] analogous to staging transitions in layer intercalates. In particular, an ordered intercalation phase (presumably metallic) coexists with pristine polymer at y values as low as 0.02, well within the soliton-doping regime.

The first evidence for phase transitions versus y in $[(CH)K_y]_x$ was provided by the electrochemical data of Shacklette and Toth;[3] anomalies in open-circuit voltage V_{OC} versus y were attributed to first-order transitions between different channel intercalation structures. *Ex situ* diffraction[4-6] demonstrated the existence of ordered phases at fixed y values, and recent *in situ* x-ray experiments clearly confirm the first-order transitions between ordered phases.[2] These data are consistent overall with a simple model for the free energy of a two-dimensional (2-D) commensurate channel superlattice,[7] while similar data for Na doping[8] were interpreted in terms of a commensurate-incommensurate transition as a function of y.

The y-dependent electronic properties of alkali-doped $(CH)_x$ [ESR (Ref. 9), conductivity (Ref. 3) susceptibility (Ref. 10)] have been extensively used as probes of structural and electronic transitions. These are generally more convenient than *in situ* diffraction and have been successfully applied to graphite intercalates as a preliminary signature of new structural transitions.[11] We take the same approach here, motivated mainly by the direct observation[2] of only a few of the predicted[3,7] structural transitions so far. A second goal is to examine the degree of correlation between the new x-ray data and previous electronic-property results. V_{OC} and conductivity $\sigma_{\parallel}$ are complementary probes. The former is directly related to the free energy and will therefore reveal structural transitions involving changes in lattice constants and/or symmetries, while $\sigma_{\parallel}$ may be sensitive to more subtle effects. For example, host chain rotations will affect $\sigma_{\parallel}$ via the interchain coupling but their contribution to the lattice energy could be masked by Coulomb interactions. Also, commensurate-incommensurate and order-disorder transitions within the intercalate channels may be unobserv-

able in V_{OC} for similar reasons but may show up in $\sigma_{\parallel}(y)$ in the metallic regime due to small changes in carrier mobility.

In this experiment we used very small steps in y to look for additional conductivity and V_{OC} anomalies which might indicate new structural transitions and to correlate with recent *in situ* ESR.[9] We also took pains to avoid problems with inhomogeneous doping,[12] to ensure near-equilibrium conditions, and to check reproducibility by multiple doping-dedoping cycles. The emphasis in this paper is on the structural aspects; a subsequent publication will discuss in detail the functional dependence of $\sigma_{\parallel}(y)$.

EXPERIMENT

We used a 1-μm thick $(CH)_x$ electrode prepared by the Akagi liquid-crystal method.[13] Raman, infrared (IR), and x-ray data are consistent with a chain-axis distribution of 40°–50° FWHM about the mean, and a fraction < 4% of randomly oriented crystalline material. Thicker films contain a sizable volume fraction of random crystalline material, presumably because the newly arriving gas cannot diffuse to the oriented substrate before polymerizing.[14] Scanning electron and optical microscopy show typical fibrillar morphology with diameters in the range 200–600 Å. The apparent distribution of fibril axes is much narrower than that of the chains. The film was assembled in a pyrex cell with potassium counter electrode and 1 mol $KB(ethyl)_3CN$ in tetrahydrofuran as the electrolyte. The $(CH)_x$ was fitted with four nickel pressure contacts to measure $\sigma_{\parallel}$ parallel to the fibrils, all held at the same potential during doping and/or dedoping to help ensure uniformity. The inital V_{OC} was 1.6–1.8 V. Increments $dy = \pm 0.002$ were imposed by a constant potential close to the equilibrium V_{OC}, and the cell was allowed to relax (open circuit) for 12 h between steps, after which dV_{OC}/dt was less than 1 mV/h. Under these conditions, a complete doping/dedoping cycle required 3 months. Two problems were encountered in establishing the y scale. The small mass < 1 mg necessitated scaling to previous data from more massive electrodes; we assigned $y=0.167$ to the charge accumulated at $V_{OC}=0.3$ V.[3] Subsequent cycles suggested a small, but significant, loss of "dopable" material since both the maximum apparent conductivity and the accumulated charge at a reference potential corresponding to this maximum decreased systematically. Thus, we rescaled the y axis as above after each doping half-cycle. This procedure implied cumulative fractional losses of 6%, 13%, and 16.5% after the second, third, and fourth doping half-cycles. This effect is much larger than the effect associated with "residual dopant," i.e., the impossibility to dedope the cell to its original V_{OC} or to retrieve the initial high resistivity of undoped $(CH)_x$. Our somewhat arbitrary procedure at least locates the previously observed strong features within 10% of their reported y values, as discussed below; we conservatively estimate a 20% margin of error in our y calibrations. Four-point conductivity was measured with the cell inverted to eliminate the electrolyte contribution, using dc currents 5–50 uA. The absolute accuracy was about ±10% while the relative accuracy versus y was considerably better.

RESULTS

Figure 1 shows V_{OC} and $\sigma_{\parallel}$ versus y for the second and fourth cycles. The overall behavior is similar to Ref. 3. The first cycle (not shown) is atypical since the low-y region during doping includes the consequences of cis → trans isomerization; $\sigma_{\parallel}$ sharply increases from its initial value 10^{-6} S/cm (characteristic of a cis-trans mixture) to 10 000 S/cm at $y=0.06$, then increases more slowly to a maximum of 17 500 S/cm at $y=0.12$,[15] decreasing slightly thereafter. The maximum occurs near $y=0.12$ for all cycles, its value dropping continuously with repeated cycling to 11 000 S/cm by the fourth cycle. We did not attempt to correct $\sigma_{\parallel}$ for the (presumed) loss of doped volume fraction. The dedoping log plots in Fig. 1 show an abrupt increase with increasing y at $y=0.02$, reaching values within a decade of the maximum already at $y=0.03$. The linear plots reveal a large hysteresis,; $\sigma_{\parallel}$ is generally larger during doping than dedoping at a given y. Overall, the hysteresis diminishes with repeated cycling (with important exceptions evident on the log plots). In addition to the global behavior just described, both linear and log plots show "fine structure," which is more pronounced during dedoping than doping. This is reminiscent of the results obtained on graphite compounds, in which anomalies in resistivity versus temperature or hy-

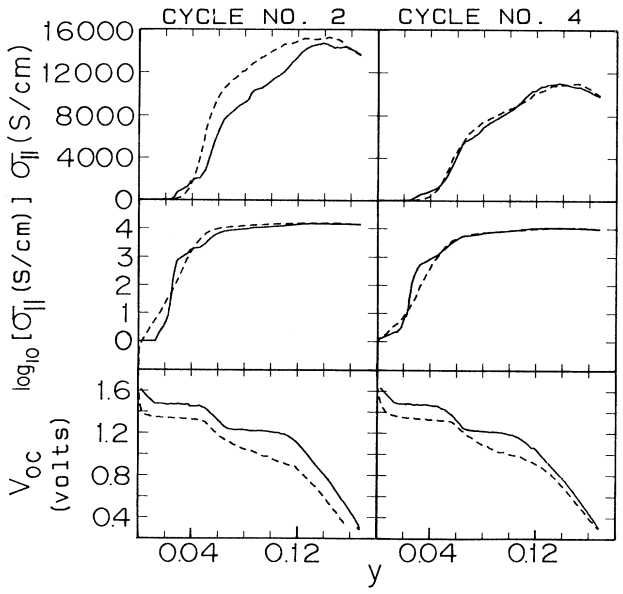

FIG. 1. Potassium-doped polyacetylene: variation of the parallel conductivity (top row: linear scale; middle row; log scale) and open-circuit voltage, (bottom row) with K concentration during doping (dashed curves) and dedoping (solid curves) for the second (left column) and fourth (right column) complete cycles.

drostatic pressure at fixed intercalate concentration[11] were subsequently identified with structural transitions.

The bottom two panels of Fig. 1 show $V_{OC}(y)$ for the second and fourth cycles. These exhibit the typical sequence of sloping regions and quasiplateaus, the dedoping half-cycles generally having larger V_{OC} at a given y, and better-defined "transitions," than the doping half-cycles. On general thermodynamic grounds, structure in $V_{OC}(y)$ is expected to reveal first-order phase boundaries between ordered intercalation phases. Regions in which both V_{OC} and y change signify the isostructural addition or subtraction of ionic charge, while the constant V_{OC} plateaus represent mixed-phase regions between neighboring ordered structures.[16] Using the now-standard notation, the large initial slope at $y=0$ is the undoped polymer, the sloping region centered near $y=0.06$ signifies "stage 2" (defined below), and the second broad sloping region in the range $0.12 < y < 0.17$ is referred to as "stage 1." The large differences in plateau voltages between doping and dedoping indicate differences in detail between phase separations which occur in the two directions. As with $\sigma_{\parallel}(y)$, we observe that the overall hysteresis in $V_{OC}(y)$ decreases continuously with repeated cycling. For the fourth cycle, hysteresis is essentially limited to the coexistence plateaus, as would be expected for an ideal intercalation electrode exhibiting a sequence of first-order transitions. In particular, doping and dedoping data points for the sloping regions representing pure stage 1 and stage 2 lie on unique straight lines, as required for a specific *equilibrium* configuration of guest sites in a host lattice.

To the extent that the isostructural addition or subtraction of charge can be represented as an effective capacitance, the model developed by Metrot and coworkers for staging transitions and "overcharging" during electrointercalation of graphite should apply.[17] An idealization of this model is shown schematically in Fig. 2(a), in which we identify the three sloping regions in $V_{OC}(y)$ with known structures. M denotes the monoclinic trans-$(CH)_x$ phase; preliminary data indicates that the lattice parameters a and b increase slightly with light doping, suggesting that this phase might possibly accommodate a small concentration of structural potassium.[18] S-2 and S-1 represent primitive and body-centered-tetragonal cells of stage 2 and stage 1, respectively, both of which are stable over a range of y due to variable channel occupancy. In Metrot's model, the slope $dV_{OC}(y)/dy$ is associated, in part, with the Fermi-level movement in a "rigid-band" metallic density of states. In $(CH)_x$, the first slope at low y should thus be larger than the others since this is the soliton-doping regime leading to the insulator $\rightarrow$ metal transition. This is what is observed. Another important observation is that, *even under very slow conditions,* the first few cycles can be affected by extrinsic hysteresis processes, near-ideal behavior occuring only after four cycles. It is also apparent from Fig. 1 that, even after four cycles and with the same doping and dedoping rate, the doping $V_{OC}(y)$ curves are less ideal than the dedoping ones—in particular, there is still appreciable variation in $V_{OC}(y)$ throughout the doping coexistence

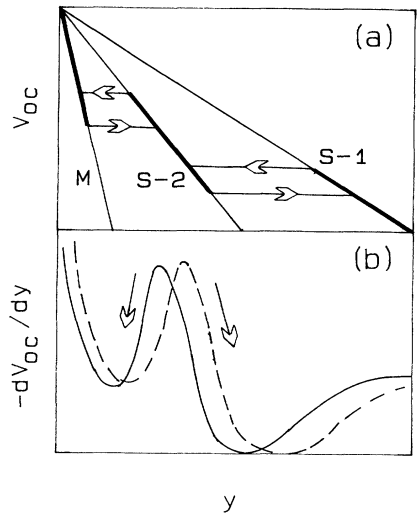

FIG. 2. Schematic representation of $V_{OC}(y)$ and $-dV_{OC}/dy$ vs y for an intercalation electrode exhibiting first-order phase transitions (after Metrot, Ref. 17). Both abcissa and ordinate scales are arbitrary.

plateaus. In a similar *in situ* x-ray-diffraction experiment, Djurado *et al.* noted that the Bragg peaks from stages 1 and 2 were much sharper on dedoping as compared to doping.[2] Both observations suggest a fundamental difference between the microscopic processes involved in doping and dedoping.

In Fig. 3 we present derivative curves $d\sigma_{\parallel}/dy$ and $-dV_{OC}/dy$ obtained numerically from the data of Fig. 1. Both exhibit major features which can be accounted for by the structural transitions implied in Fig. 2(a). Both also show additional "fine structure" suggestive of new

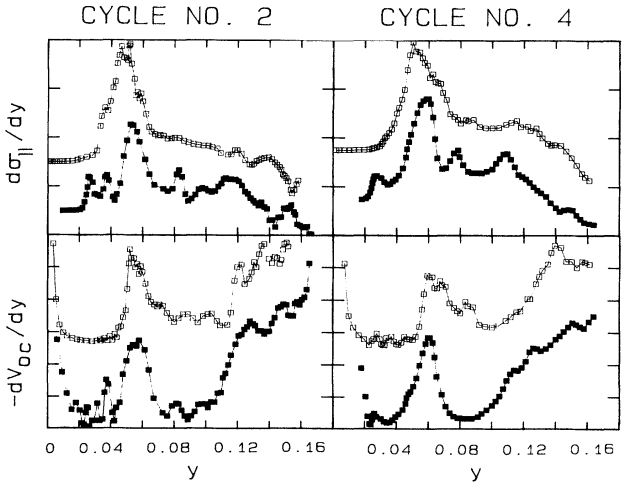

FIG. 3. Numerical derivatives with respect to mole fraction y of the Fig. 1 data. Open and solid squares for doping and dedoping, respectively. Solid lines are guides to the eye, and the abcissa scales are arbitrary.

transitions. In general, the dedoping curves are richer than the doping ones, and $d\sigma_{\parallel}/dy$ shows more singularities than $-dV_{OC}/dy$. Overall, $-dV_{OC}/dy$ agrees with the idealization shown in Fig. 2(b), including most aspects of the predicted intrinsic hysteresis. The most prominent feature in all the curves is a peak at $0.052 < y < 0.058$ on our corrected y scale, ascribed to pure stage 2 and consistent within our stated error with Ref. 3. The second prominent feature is the more-or-less abrupt increase in $-dV_{OC}/dy$ at $y > 0.10$ which signals the onset of pure stage 1; extrapolating this feature to the noise level indicates that pure stage 1 is achieved at $y = 0.12$ and 0.10 for doping and dedoping, respectively. As expected, $d\sigma_{\parallel}/dy$ shows a strong peak at the transition between M and stage 2 but only a weak one at the stage 2 $\rightarrow$ stage 1 transition.

Additional weak features are observed in all three y regions separating the known pure phases and will be discussed accordingly. Between M and stage 2 ($0 < Y < 0.06$), $d\sigma_{\parallel}/dy$ shows a peak at 0.028 in all four cycles and a similar peak at 0.034–0.038 in cycle Nos. 2 and 3, but only on dedoping. Cycle No. 2 data in Fig. 3 (top left panel) suggest that these may be present as unresolved shoulders during doping. Very weak evidence for similar structures in $-dV_{OC}/dy$ upon dedoping is present in cycle Nos. 2 and 4; in contrast, $-dV_{OC}/dy$ is featureless during all four doping half-cycles. The ESR linewidth also exhibits a discontinuity in this y range.[9]

Several features are observed between pure stage 2 and the onset of stage 1 ($0.06 < y < 0.10$). For dedoping cycle No. 2 (Fig. 3, lower left panel), $-dV_{OC}/dy$ shows a clear peak at 0.080 and a weaker one at 0.096; the corresponding doping curve has similar features at slightly higher y values suggestive of hysteresis. These are also found in dedoping cycle No. 1 but not in No. 3; No. 4 shows only the lower one, and only during doping (Fig. 3, lower right). Both features show up variously in $d\sigma_{\parallel}/dy$; all four dedoping cycles exhibit a peak at 0.080–0.083 while Nos. 1 and 2 show evidence for the second one at 0.090 and 0.095, respectively, and weak evidence for the 0.080 peak is found during doping cycle Nos. 2 and 4 (top panels, Fig. 3). This range also exhibits a second plateau in ESR linewidth.[9]

The onset of pure stage 1 gives rise to the large increase in $-dV_{OC}/dy$ beginning at about 0.12 and 0.10 for doping and dedoping, respectively. Broad and weak features in $d\sigma_{\parallel}/dy$ occur at roughly corresponding y values. All but the first dedoping cycle show clear evidence in $-dV_{OC}/dy$ for additional features at about 0.12 and 0.15; similar, but nonreproducible, effects occur on doping. The dedoping features are replicated in $d\sigma_{\parallel}/dy$; for example, cycle No. 2 shows a broad peak just below 0.12 and a sharper one centered at 0.152 (Fig. 3, top left). A third ESR plateau is found in this y range.[19]

At this stage, the identification of new singularities is not as firm as one would like. Even allowing 12 h after y increments of 0.002 (the data in Figs. 1 and 3 took a year to accumulate), reproducibility from cycle to cycle is far from perfect. There also appears to be a fundamental difference between doping and dedoping which makes it

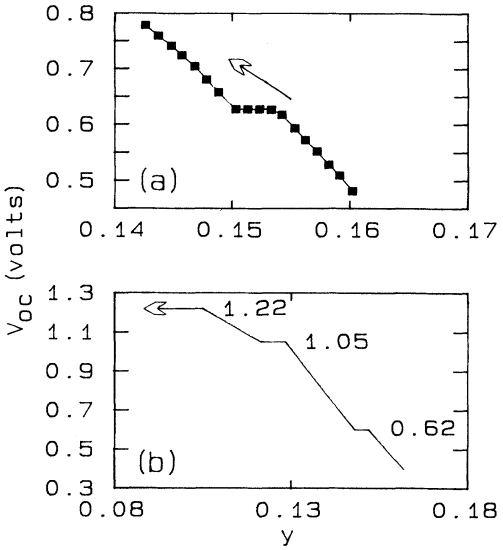

FIG. 4. (a) Detailed measurement of $V_{OC}(y)$ around the 0.62-V dedoping plateau; (b) schematic summary of several such measurements showing the existence of three pure stage-1 phases.

difficult to "align" features obtained in both directions, even accounting for the intrinsic (ideal) hysteresis. In order to partly clarify matters, we performed a few additional experiments over limited V_{OC} ranges with even smaller steps and longer relaxation times, especially to confirm the existence of multiple V_{OC} singularities within the presumed pure stage-1 regime. By crossreferencing the y locations of $-dV_{OC}/dy$ singularities (Fig. 3) with the $V_{OC}(y)$ data (Fig. 1), we identified V_{OC} ranges to study more carefully. For example, the dedoping $-dV_{OC}/dy$ singularity at 0.15 implies the existence of a plateau in V_{OC} near 0.6 V which is not evident in Fig. 1. Using a finer mesh and longer relaxation, we have indeed observed such a plateau directly at 0.61 and 0.63 V in two separate experiments; the results of the latter are shown in Fig. 4(a). Similarly, the derivative peak at $y = 0.12$ demands a V_{OC} plateau near 1.1 V, which is barely visible in dedoping cycle No. 4 but shows up clearly at 1.05 V in a detailed search. Using the same y calibration as before, we can locate these features as follows. The 0.6 V plateau extends from 0.148 to 0.152, and the 1.05-V plateau runs from 0.121 to 0.128; the major plateau at 1.22 V covers the range $0.065 < y < 0.102$ (cycle No. 4, Fig. 1), all values referring to dedoping. In light of Ref. 2, these new plateaus imply the existence of three distinct stage 1 phases, all with the same basic channel structure. In Fig. 4(b) we assemble all the $V_{OC}(y)$ results into a schematic composite of the stage 1 dedoping regime. Obviously the three implied phases do not fit the Metrot model, the two more concentrated ones exhibiting larger, not smaller, slopes than the phase of lowest concentration.

All of the features we find in $-dV_{OC}/dy$ are generally consistent with Ref. 3, while the direct observation of

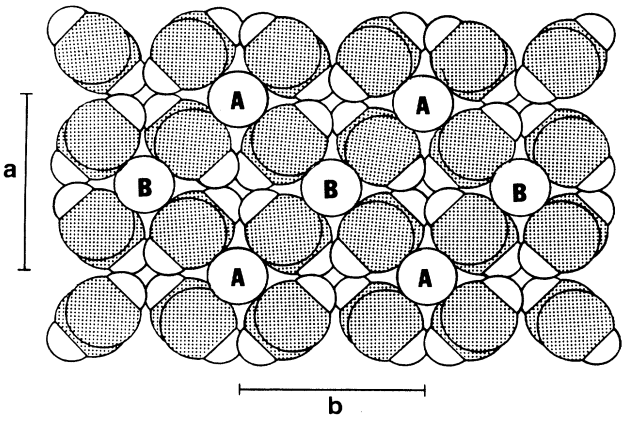

FIG. 5. Channel structures for stage-1 and stage-2 potassium-doped $(CH)_x$ (Refs. 2 and 6). The corner channels A are selectively occupied first, leading to a primitive tetragonal stage-2 cell; further doping is achieved by filling the center B channel. Pure stage 1 consists of equal filling of both. The lattice parameter a expands from 8.2 to 8.4 Å as the B channels fill up (Ref. 2).

V_{OC} plateaus at 1.05 and 0.62 V is new. The $d\sigma_{\parallel}/dy$ curves also give strong evidence for a new effect near $y=0.03$ which is also seen in ESR. Assuming that each feature is associated with a unique phase, then there are at least six such phases, only two of which have been directly identified in diffraction experiments.

DISCUSSION

The original proposal for staging in alkali-doped $(CH)_x$ (Ref. 3) was based on the assumption of three-dimensionally ordered and commensurate intercalate sublattices, consisting of channels defined by m (CH) chains per channel in the (a,b) plane and n (CH) units per alkali ion along the c direction. Stable phases were thus assumed to be limited to stoichiometric compositions with integers n and m, viz., $[(C_nH_n)_mM]_x$, or $[(CH)M_y]_x$ with $y=1/nm$. This assumption must be viewed in light of the $V_{OC}(y)$ data which imply that pure phases exist on continua of y values, and in the context of x-ray results showing the persistence of unique 2D channel superlattices over *the same continua of y's*. The assumption may be reconciled with the facts by arguing that m and n represent "hard" and "soft" degrees of freedom, respectively; that is, the internal energy of a given phase is dominated by interchain (CH)-(CH) and interchannel M-M interactions, while the (CH)-M and intrachannel M-M interactions are much weaker. A good example of similar competing interactions in the obverse dimensionality is provided by the work of Bouyad *et al.* on graphite bisulfate.[19] Here $V_{OC}(y)$ shows four sloping regions and three plateaus associated with transitions between 1D staging superlattices, the pure stage-2 slope covering a range C_{21}^{+} to C_{28}^{+} of charge on the graphite electrode. X-ray diffraction shows that the in-plane intercalate structure *and* the 3D correlations between guest and host sublattices exhibit several transitions throughout the pure stage 2 regime, but there is no evidence of these transitions in $V_{OC}(y)$. In this system the 1D staging superlattice is the "hard" degree of freedom while the 2D intercalate structure and its coupling to the host are "soft;" the internal energy is dominated by interlayer interactions while the nature of the intercalate layer (ordered, disordered, commensurate) has an unobservably small effect on the cell potential. While specific 3D ordered phases exist at unique values of charge, each basic superlattice structure is able to accomodate a range of charge before transforming to a new periodicity. Given the similarities in $V_{OC}(y)$ between the two systems, and the analogy between persistent 1D layer sequences and 2D channel structures, we are led to apply the same notions in discussing the present results.

It is generally agreed that the basic channel structure for $[(CH)K_y]_x$ is as shown in Fig. 5, and that doping from $y=0$ to 0.17 consists of the selective occupation first of the corner channels in the tetragonal cell (stage 2), followed by filling the central channels (stage 1).[20] Thus, the stage-2 $\rightarrow$ stage-1 transition is achieved by m decreasing from 4 to 2. The x-ray data of Ref. 2 show clearly that the channel structures for $[(CH)K_y]_x$ can be described with only these two m values over the entire y range; in particular, there is no evidence for (a,b) plane disorder or incommensurability at any y. Thus, if any phases other than stage 2 and stage 1 exist, they must involve variations in n. The highest concentration $y=0.167$ occurs at $n=3$, $m=2$. This is a stage-1 phase ("1C") with intrachannel K-K distance 3.7 Å, presumed to be the hard-sphere limit for strictly 1D columns. Referring to Fig. 4(b), this phase survives upon dedoping to $y=0.152$, i.e., 9% vacant sites in the (implied) commensurate structure. Further removal of potassium triggers the emergence of a more dilute stage 1 phase "1B" (onset of the plateau at 0.62 V) which coexists with "1C" over a very narrow range of y centered at 0.150. Further dedoping leads to the pure "1B" sloping region $0.128<y<0.148$ which, given our y error, probably includes the next stoichiometric composition $n=4$ ($y=0.125$). Increasing V_{OC} to 1.05 V (second plateau), a third stage "1A" appears, coexisting with "1B" down to $y=0.122$ and existing as a pure phase down to 0.106 thus probably including $n=5$. Below $y=1.06$ we enter the major plateau at 1.22 V signifying the onset of stage 2. The dedoping $d\sigma_{\parallel}/dy$ curves in Fig. 3 show weak negative extrema at 0.145 and 0.16, which coincide approximately with the midpoints of pure 1B and 1C, respectively. In contrast, pure 1A seems to correlate with a positive extremum in $d\sigma_{\parallel}/dy$ near $y=0.11$. It is possible that these weak conductivity extrema are associated with the three stoichiometric stage-1 compositions.

Figure 4(b) indicates that, in contrast to graphite bisulfate, the different intrachannel densities of the three stage-1 phases cannot be regarded as belonging to essentially the same equilibrium structure. Coexistence plateaus occur within the same underlying 2D superlattice, and the three slopes differ qualitatively from the predic-

tion of the isostructural capacitance model Fig. 3(b). One possibility is that the energy associated with commensurate lock in along the c direction is large enough to stabilize distinct 3D structures with identical 2D channel lattices. A similar phenomenon occurs in Li graphite; the guest-host interaction is sufficiently strong to stabilize two distinct in-plane structures (one of which is disordered) with the same stage-2 layer superlattice at 300 K.[21] A second possibility is that the disposition of the (CH) chains about the channels is density dependent for a given 2D channel superlattice. In fact, the x-ray data of Saldi *et al.*[6] and a reanalysis of our *in situ* x-ray data,[20] both for $y=0.12$, are inconsistent with the highly symmetric stage-1 arrangement shown in Fig. 5, leaving open the possibility of different chain arrangements for the same channel structure. A third possibility is that one or more of the stage-1 phases is disordered along the c axis (as suggested by the x-ray data[2]), which might also explain the reversible decrease in $\sigma_{\parallel}$ in the range $0.12<y<0.17$ which must therefore be associated with a reversible structural phenomenon. As stated above, the only degree of freedom in this y range is the density along the c axis. It is then reasonable to suggest that the decrease in $\sigma_{\parallel}$ with increasing y is a consequence of the evolution from stage $1A$ to stage $1C$. We point out that a similar decrease in conductivity with increasing concentration is observed in most graphite compounds, stage 2 typically having higher σ than stage 1.[22]

The width of the 1.22-V plateau indicates that stage 1 coexists with stage 2 down to $y=0.065$ upon dedoping, at which point only the stage-2 channel structure (Fig. 5) is observed in the diffraction profile.[2] The singularity observed at $y=0.08$ in some of the dedoping derivative curves is most likely a kinetic effect, due either to metastable, very dilute stage 1 ($m=2$, $n=6$) or to the first appearance of stage 2 with (metastably) close-packed K ions ($m=4$, $n=3$).[3] It is unlikely that either of these exist in equilibrium since we do not observe multiple V_{OC} plateaus analogous to Fig. 4(b). Pure stage 2 exists over a much narrower range than stage 1, $0.05<y<0.065$. The only example of an in-plane close-packed stage-2 graphite compound is $Li_{0.5}C_6$; more typically the stage-2 alkali-metal compounds exhibit lower in-plane densities at ordinary temperature and pressure than their stage-1 counterparts.[21]

Finally, we consider the derivative features around $y=0.03$. The most prominent feature in V_{OC}, $\sigma_{\parallel}$, and ESR linewidth[9] occurs within the pure stage-2 regime at $y=0.06$. The x-ray data[2] clearly show that the stage-2 channel structure persists down to $y=0.02$, and the 1.4-V coexistence plateau between stage-2 and undoped trans extends below $y=0.02$. Thus, as with the stage-1 regime, we propose the existence of "dense" and "dilute" stage 2's. The "dense" variety accounts for the prominent features in all the experiments, and includes the stoichiometric composition $m=n=4$.[3] The analogous Li-graphite phase is Li_xC_6, $x=0.5$;[21] the Li-C interactions are sufficient to stabilize a nonstoichiometric "dilute stage 2" with $0.3<x<0.4$, having the same 1D superlattice but only $\approx 70\%$ site occupancy within a gallery. It is tempting to attribute the dedoping $d\sigma_{\parallel}/dy$ anomaly at $y=0.03$ to a corresponding "dilute stage-2" channel structure with $n\sim 8$. It is significant that the ESR linewidth also shows an anomaly, only upon dedoping, at $y=0.03$.[9] These anomalies have been attributed to structural effects by arguing that the width depends on the conduction electron residence time near a dopant site (consistent with its dependence on dopant mass) and is thus sensitive to the density and geometrical arrangement of occupied sites. The absence of the $y=0.03$ anomaly during doping, as well as the lack of a corresponding step in $V_{OC}(y)$, might imply that this is not an equilibrium phase but rather a transition state during the evolution from pure (dense) stage 2 to trans.

The overall behavior of $\sigma_{\parallel}(y)$ confirms that the transition from undoped $(CH)_x$ to stage 2 has much more dramatic electronic consequences than the stage-2 $\rightarrow$ stage-1 transition—10 decades versus a factor of 1.7, respectively (probed by ESR linewidth, the corresponding changes are factors of 40 and 1.4). Interpreting the conductivity enhancement in the range $0<y<0.06$ in terms of coexisting insulating and conducting phases is complicated by (i) the possibility that the trans-$(CH)_x$ cell parameters at low y are dilated from their $y=0$ values, suggestive of random channel doping rather than strictly neutral material coexisting with "metallic" stage 2,[18] and (ii) our observation of large hysteresis in $\sigma_{\parallel}(y)$ including the possibility of a metastable structure with some intermediate *local* y value. The high-resolution $V_{OC}(y)$ and $\sigma_{\parallel}(y)$ data presented here should provide a useful guide for more detailed diffraction studies designed to shed light on these issues. Our suggestions here imply that *in situ* $(00L)$ scans using oriented $(CH)_x$ will be most informative.

ACKNOWLEDGMENTS

We acknowledge useful conversations with Paul A. Heiney. This work was supported by Department of Energy (DOE), Grant No. DEFG02-87ER45254 (JEF) and by North Atlantic Treaty Organization (NATO) Grant No. 0866/87.

[1]A. J. Heeger, S. Kivelson, J. R. Schrieffer, and W. P. Su, Rev. Mod. Phys. **80**, 781 (1988).
[2]D. Djurado, J. E. Fischer, P. A. Heiney, J. Ma, N. Coustel, and P. Bernier, Synth. Met. **34**, 683 (1990).
[3]L. W. Shacklette and J. E. Toth, Phys. Rev. B **32**, 5892 (1985).
[4]N. S. Murthy, L. W. Shacklette, and R. H. Baughman, Phys. Rev. B **41**, 15 (1990).
[5]O. Leitner, H. Kahlert, G. Leising, J. Fink, and H. Fritzsche, Synth. Met. **28**, D225 (1989).
[6]F. Saldi, J. Ghanbaja, D. Begin, M. Lelaurain, and D. Billaud, C. R. Acad. Sci. **309**, 671 (1989).
[7]J. Ma, H.-Y. Choi, E. J. Mele, and J. E. Fischer, Synth. Met. **27**, A75 (1988).
[8]M. Winokur, Y. B. Moon, A.J. Heeger, J. Barker, D. C. Bott,

and H. Shirakawa, Phys. Rev. Lett. **58**, 2329 (1987).

[9]C. Fite and P. Bernier, Phys. Rev. B **36**, 4574 (1987); N. Coustel, C. Fite, and P. Bernier, Mater. Sci. Forum **42**, 143 (1989).

[10]J. Chen and A. J. Heeger, Synth. Met. **24**, 311 (1988).

[11]C. D. Fuerst, D. Moses, and J. E. Fischer, Phys. Rev. B **24**, 7471 (1981); D. G. Onn, G. M. T. Foley, and J. E. Fischer, *ibid.* **19**, 6474 (1979).

[12]B. Francois, C. Mathis, and R. Nuffer, Synth. Met. **20**, 311 (1987).

[13]K. Akagi, S. Katayama, H. Shirakawa, K. Ataya, A. Mukoh, and T. Narahara, Synth. Met. **17**, 241 (1987).

[14]A. Montaner, M. Rolland, J. L. Sauvajol, L. Meynadier, R. Almairac, J. L. Ribet, M. Galtier, and C. Grill, Synth. Met. **28**, D19 (1989); N. Coustel, N. Foxonet, J. L. Ribet, P. Bernier, J. E. Fischer, and P. A. Heiney (unpublished).

[15]In analogy with mechanically stretched $(CH)_x$ [A. G. MacDiarmid and A. J. Heeger, in *Molecular Metals,* edited by W. E. Hatfield (Plenum, New York, 1979), p. 161] and using 450 *S*/cm for unoriented K-doped $(CH)_x$ (Ref. 3), our pseudoepitaxial sample exhibits a $\sigma_{\|}$ equivalent to a draw ratio $L/L_0=6$.

[16]A. Metrot and J. E. Fischer, Synth. Met. **3**, 201 (1981).

[17]A. Metrot, Synth. Met. **7**, 177 (1983); A. Metrot and M. Tihli, *ibid.* **12**, 517 (1985); **23**, 19 (1988).

[18]P. A. Heiney, J. E. Fischer, D. Djurado, J. Ma, N. Coustel, and P. Bernier, Bull. Am. Phys. Soc. **35**, 242 (1990). This work is still in progress.

[19]B. Bouyad, H. Fuzellier, M. Lelaurain, A. Metrot, and F. Rousseaux, Synth. Met. **7**, 325 (1983).

[20]Detailed x-ray work shows that the highly symmetric arrangement of chains and channels in Fig. 5 is not correct [see Ref. 6; also J. E. Fischer, P. A. Heiney, and J. Ma, Synth. Met. (to be published); P. A. Heiney, J. E. Fischer, D. Djurado, J. Ma, D. Chen, M. Winokur, N. Coustel, P. Bernier, and F. A. Karasz (unpublished)]. This has only a secondary effect on the interpretation of the present results.

[21]J. E. Fischer, in *Chemical Physics of Intercalation,* edited by A. P. Legrand and S. Flandrois (Plenum, New York, 1987), p. 59.

[22]See, for example J. E. Fischer and T. E. Thompson, Phys. Today **35**, (1978).